

On Throughput Region for Primary and Secondary Networks With Node-Level Cooperation

Xu Yuan, *Member, IEEE*, Feng Tian, *Member, IEEE*, Y. Thomas Hou, *Fellow, IEEE*, Wenjing Lou, *Fellow, IEEE*, Hanif D. Sherali, Sastry Kompella, *Senior Member, IEEE*, and Jeffrey H. Reed, *Fellow, IEEE*

Abstract—Cooperation has become an essential element in spectrum sharing between the primary and secondary networks. A new trend in cooperation is to allow the primary and secondary networks to cooperate on the node level for data forwarding. This new paradigm allows to pool network resources from both the primary and secondary networks and allows users in each network to access a much richer network infrastructure in a combined network. This paper offers an in-depth study of such node-level cooperation by explaining its optimal throughput curve—the maximum achievable throughput for both the primary and secondary users. We formulate the problem as a multicriteria optimization problem with the goal of maximizing the throughput of both the primary and secondary users. Through a novel approach based on weighted Chebyshev norm, we transform the multicriteria optimization problem into a single criteria optimization problem and find a sequence of Pareto-optimal points iteratively. Based on the Pareto-optimal points, we construct the throughput curve and show that it provides an ϵ -approximation to the optimal curve. We prove some important properties of the optimal throughput curve. Through a case study, we show that the throughput region (the area under the throughput curve) under node-level cooperation is substantially larger than that when there is no node-level cooperation.

Index Terms—Spectrum sharing, cooperation, throughput region, multiobjective optimization, primary network, secondary network.

I. INTRODUCTION

RECENT push by the government agencies to share federal government radio spectrum with non-government entities has fueled the development of innovative technologies for spectrum sharing [13]. Coexistence of a secondary network with the primary network is the key to improve radio spectrum

Manuscript received May 7, 2016; revised August 5, 2016; accepted August 28, 2016. Date of publication September 2, 2016; date of current version October 13, 2016. This work was supported in part by NSF under Grants 1642873, 1617634, 1443889, 1343222 and in part by ONR under Grant N00014-15-1-2926. The work of S. Kompella was supported in part by the ONR. This work was completed while X. Yuan was with the Virginia Polytechnic Institute and State University. This paper was presented in part at IEEE DySPAN, Stockholm, Sweden, September 29–October 2, 2015 [21].

X. Yuan was with Virginia Polytechnic Institute and State University, Blacksburg, VA 24061 USA. He is now with University of Toronto, Toronto, ON M5S 3G4, Canada (e-mail: xuyuan@ece.utoronto.ca).

Y. T. Hou, W. Lou, H. D. Sherali, and J. H. Reed are with Virginia Polytechnic Institute and State University, Blacksburg, VA 24061 USA (e-mail: thou@vt.edu; wjlou@vt.edu; hanifs@vt.edu; reedjh@vt.edu).

F. Tian is with Nanjing University of Posts and Telecommunications, Nanjing 210003, China (e-mail: tianf@njupt.edu.cn).

S. Kompella is with the U.S. Naval Research Laboratory, Washington, DC 20375 USA (e-mail: sastry.kompella@nrl.navy.mil).

Color versions of one or more of the figures in this paper are available online at <http://ieeexplore.ieee.org>.

Digital Object Identifier 10.1109/JSAC.2016.2606018

utilization. There has been extensive research on exploring coexistence between the primary and secondary networks in recent years. Goldsmith *et al.* [7] outlined three coexistence paradigms, namely *interweave*, *underlay*, and *overlay*. These three paradigms were defined from an *information theoretic* perspective, solely based on how much side information (e.g., channel conditions, codebooks) is available to the secondary users. In the networking community, these three paradigms have been mapped into specific scenarios of how primary and secondary networks interact with each other for data forwarding. Specifically, the *interweave* paradigm refers to the simple idea that the secondary users are allowed to use a spectrum band allocated to the primary users only when the primary users are not using the band [1], [6], [18], [23]. This is the simplest approach to meet the current FCC requirements, which mandate that secondary users shall not produce interference that is harmful to the primary users. This paradigm is analogous to the classic interference avoidance in medium access, or in cognitive radio (CR) terminology, *dynamic spectrum access* (DSA). This is the prevailing scenario to which most of research efforts have been devoted by the CR research community in recent years. The *underlay* paradigm refers to that secondary users' activities or interference on primary users is negligible (or below a given threshold). In contrast to the *interweave* paradigm, secondary users may be active *concurrently* with the primary users in the same area and in the same channel as long as the interference produced by the secondary nodes are controlled below a certain threshold (e.g., noise level). This can be achieved through a systematic interference cancelation (IC) by the secondary nodes without noticeable impact on the primary nodes [2], [5], [10], [20], [24], [25]. Finally, the *overlay* paradigm refers to having the secondary users offer some levels of cooperation with the primary users in data forwarding [8], [9], [11], [12], [15], [17], [22].

Under the *interweave* and *underlay* paradigms, the primary network would not feel the presence of the secondary network. The primary and secondary networks are independent in terms of data forwarding in each network. However, under the *overlay* paradigm, there is a certain level of cooperation on the data plane by the secondary network. Inspired by this cooperation idea in the *overlay* paradigm, there have been some recent efforts on how to exploit possible cooperation from the secondary users to help forward data for the primary users [8], [9], [11], [12], [15], [17], [22]. So far, these efforts have been limited to only having the secondary nodes help relay primary users' traffic. There is no consideration of the converse (i.e., primary users helping the secondary users), or

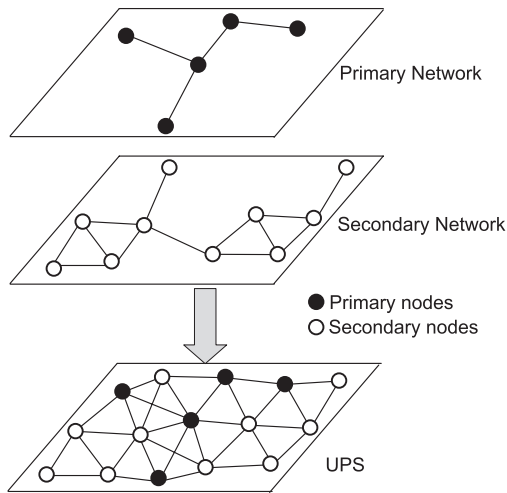


Fig. 1. An illustration of the UPS policy for multi-hop primary and secondary networks.

a broader vision of a policy-based cooperation between the two networks. Such a limitation is mainly due to current FCC rules on existing wireless services and applications.

Recently, we proposed a novel policy-based cooperation between the primary and secondary networks [19]. We proposed to employ the *node-level (data plane) cooperation* as a new dimension for spectrum sharing between the primary and secondary users. Such network cooperation can be defined by a set of *policies* under which different degrees of cooperation can be achieved. Corresponding to each cooperation policy, a traffic-forwarding behavior for the primary and secondary users can be defined. A primitive policy used in [8], [9], [11], [12], [15], [17], and [22] is to have the secondary network help relay primary users' traffic. Another policy, called UPS [19], is to allow complete node-level cooperation between the primary and secondary networks for data forwarding. These two examples are among many possible policies that one can define to achieve network sharing between the primary and secondary networks.

Figure 1 illustrates the UPS policy for a multi-hop primary and secondary network. It allows complete cooperation between the two networks on the data plane to help relay each other's traffic. Unlike the primitive policy, which is limited to only allowing secondary nodes help relay primary nodes' traffic, UPS allows primary nodes to help relay secondary nodes' traffic. From a network infrastructure perspective, the UPS policy allows to pool all the resources from both the primary and secondary networks together so that users in each network can access a much richer network infrastructure in a combined network. Note that although the two networks are combined into one at the node level, priority or service guarantee to the primary network traffic can still be enforced by implementing appropriate traffic engineering objectives. There are many potential benefits for node-level (data plane) cooperation between the primary and secondary networks. From the network perspective, the improved network connectivity, increased flexibility in power control, scheduling and routing all translate into improved forwarding performance for primary and secondary users' traffic. From a spectrum-sharing

perspective, the ability to access other network infrastructure helps improve spatial diversity, thus allowing users to tap unused resources in the spatial domain. From an economic perspective, node-level sharing reduces the cost of building independent infrastructures for the primary and secondary networks. The UPS policy is ahead of today's FCC policies. But the benefits it offers may justify and propel it to become a viable approach for cooperation between the primary and secondary networks.

In this paper, we offer an in-depth study of throughput performance for the UPS policy. In [19], we studied the maximum throughput for the secondary users while guaranteeing the rate requirement of the primary users. The proposed solution allows us to find a single point (a pair of throughput values for the primary and secondary users). Such a single-point solution does not offer a global view on the achievable throughput region between the primary and secondary users. In this paper, we are interested in exploring the throughput region for users in the primary and secondary networks. Such a region (area) is bounded by the optimal throughput curve, which gives the maximum achievable throughput for users in the secondary (primary) network for *any* user throughput requirement in the primary (secondary) network. In other words, instead of having a single-point solution, the optimal throughput curve offers the entire landscape of maximum achievable throughput for both the primary and secondary users. Such a curve cannot be constructed by connecting discrete points found by the single-point solution approach in [19] since such an approach does not offer any optimality guarantee of the connected curve. As a result, a new solution method must be developed to find the optimal throughput curve.

The main contribution of this paper is the development of a solution to find the optimal throughput curve and thus, the throughput region under the curve. To do this, we formulate a *multiobjective* optimization problem that maximizes the throughput for both the primary and secondary users. We show how to transform this multiobjective problem into a single-objective problem by using a novel approach called *weighted Chebyshev norm* [3], [14], [16]. For the transformed single-objective program, we exploit its mathematical structure, and propose a method to find new Pareto-optimal points iteratively. When the total number of Pareto-optimal points is not large, our algorithm can find all Pareto-optimal points. The throughput curve obtained from these Pareto-optimal points will be the exact optimal throughput curve. When the number of Pareto-optimal points is large, we present a termination condition upon which the final throughput curve is an ε -approximation to the optimal curve meaning that the approximation error is no more than ε – a predefined approximation error. We conduct a case study to demonstrate how to find all Pareto-optimal points iteratively and how to construct the optimal throughput curve by our algorithm. For each point on this throughput curve, we show how to construct a feasible solution based on the solution of its corresponding Pareto-optimal point. By comparing the throughput region (the area under the throughput curve) between the UPS policy and interweave, we show that the throughput region under the UPS policy is substantially larger than that under interweave.

TABLE I
NOTATION

Primary Network	
$\hat{\mathcal{N}}_P$	The set of primary nodes
$\hat{\mathcal{L}}$	The set of primary sessions
$\hat{f}_{ij}(l)$	The flow rate traversing on link (i, j) that is attributed to primary session $l \in \hat{\mathcal{L}}, i, j \in \mathcal{N}$
$\hat{s}(l)$	The source node of primary session $l \in \hat{\mathcal{L}}$
$\hat{d}(l)$	The destination node of primary session $l \in \hat{\mathcal{L}}$
$\hat{r}(l)$	The data rate achieved by primary session $l \in \hat{\mathcal{L}}$
\hat{r}_{\min}	The minimum data rate among all primary sessions
Secondary Network	
\mathcal{N}_S	The set of secondary nodes
\mathcal{L}	The set of secondary sessions
$f_{ij}(m)$	The flow rate traversing on link (i, j) that is attributed to secondary session $m \in \mathcal{L}, i, j \in \mathcal{N}$
$s(m)$	The source node of secondary session $m \in \mathcal{L}$
$d(m)$	The destination node of secondary session $m \in \mathcal{L}$
$r(m)$	The data rate achieved by secondary session $m \in \mathcal{L}$
r_{\min}	The minimum data rate among all secondary sessions.
Combined Network	
\mathcal{N}	The set of all nodes in the network, $\mathcal{N} = \hat{\mathcal{N}}_P \cup \mathcal{N}_S$
C_{ij}^b	The link capacity of link $(i, j), i, j \in \mathcal{N}$
$x_{ij}^b(t)$	= 1 if node i is transmitting data to node j in time slot t on channel b , and is 0 otherwise
\mathcal{T}_i	The set of nodes that are located within the transmission range of node $i \in \mathcal{N}$
\mathcal{I}_i	The set of nodes that are located within the interference range of node $i \in \mathcal{N}$
T	The number of time slots in a frame
\mathcal{B}	The set of available channels in the network

The remainder of this paper is organized as follows. In Section II, we present the mathematical model for the primary and secondary networks with node-level cooperation. We also present a multiobjective formulation for maximizing both the primary and secondary users' throughput. In Section III, we develop an efficient algorithm to find an ε -approximation to the optimal throughput curve for the throughput region. Section IV presents results for a case study and Section V concludes this paper.

II. MATHEMATICAL MODELING AND FORMULATION

A. Network Model

We consider a multi-hop secondary network co-located with a multi-hop primary network. Denote the set of primary nodes as $\hat{\mathcal{N}}_P$ and the set of secondary nodes as \mathcal{N}_S . Denote \mathcal{N} as the combined set of nodes from both networks, i.e., $\mathcal{N} = \hat{\mathcal{N}}_P \cup \mathcal{N}_S$. We assume there is a set of channels \mathcal{B} available in the primary network. Suppose that there are T time slots in each time frame. Denote $\hat{\mathcal{L}}$ and \mathcal{L} as the set of primary and secondary user sessions, respectively. For each primary session $l \in \hat{\mathcal{L}}$, denote $\hat{r}(l)$ as the data rate of this session l . Likewise, for each secondary session $m \in \mathcal{L}$, denote $r(m)$ as the data rate of this session m . The primary and secondary networks are allowed to share their nodes, in addition to channels. The goal of this paper is to find the optimal throughput curve for users in the primary and secondary networks. In contrast, the objective in [19] is only to maximize secondary network throughput with a fixed primary network throughput requirement. In other words, the solution in [19] only constitutes a single-point in the optimal throughput curve in this paper. Table I lists notation in this paper.

B. Interference Modeling

In the combined network, denote \mathcal{T}_i as the set of nodes in \mathcal{N} (including both the primary and secondary nodes) that is located within node i 's transmission range, where i can be either a primary or secondary node (i.e., $i \in \mathcal{N}$). If node i is in the transmission range of a node j , then node j is also in the transmission range of node i . Denote \mathcal{I}_j as the set of nodes in \mathcal{N} (including both primary and secondary nodes) that is located within node j 's interference range, where j can be either a primary or secondary node (i.e., $j \in \mathcal{N}$).

1) *Self-Interference Constraints*: We assume scheduling is done on both channels and time slots. We use a binary variable $x_{ij}^b(t), i, j \in \mathcal{N}, b \in \mathcal{B}$ and $1 \leq t \leq T$, to indicate whether node i transmits data to node j on channel b in time slot t . That is,

$$x_{ij}^b(t) = \begin{cases} 1 & \text{If node } i \text{ transmits data to node } j \text{ on} \\ & \text{channel } b \text{ in time slot } t; \\ 0 & \text{otherwise.} \end{cases}$$

where $i \in \mathcal{N}, j \in \mathcal{T}_i, b \in \mathcal{B}$, and $1 \leq t \leq T$.

Since each primary or secondary session is unicast, node i only needs to transmit to or receive from one node on a channel and in a time slot. We have:

$$\sum_{j \in \mathcal{T}_i} x_{ij}^b(t) \leq 1 \quad (i \in \mathcal{N}, b \in \mathcal{B}, 1 \leq t \leq T), \quad (1)$$

$$\sum_{k \in \mathcal{T}_i} x_{ki}^b(t) \leq 1 \quad (i \in \mathcal{N}, b \in \mathcal{B}, 1 \leq t \leq T). \quad (2)$$

Assuming half-duplex at each node i , then we have:

$$x_{ij}^b(t) + x_{ki}^b(t) \leq 1 \quad (i \in \mathcal{N}, j, k \in \mathcal{T}_i, b \in \mathcal{B}, 1 \leq t \leq T). \quad (3)$$

The three constraints in (1), (2) and (3) can be replaced by the following single and equivalent constraint:

$$\sum_{j \in \mathcal{T}_i} x_{ij}^b(t) + \sum_{k \in \mathcal{T}_i} x_{ki}^b(t) \leq 1 \quad (i \in \mathcal{N}, b \in \mathcal{B}, 1 \leq t \leq T). \quad (4)$$

2) *Mutual Interference Constraints*: For any primary or secondary node $j \in \mathcal{N}$ that is receiving data on channel b in time slot t , it shall not be interfered by another (unintended) transmitting node $p \in \mathcal{I}_j$ on the same channel and time slot. We have the following mutual interference constraint:

$$x_{ij}^b(t) + x_{pk}^b(t) \leq 1, \quad (5)$$

where $i \in \mathcal{T}_j, p \in \mathcal{I}_j, k \in \mathcal{T}_p, j \in \mathcal{N}, j \neq k, b \in \mathcal{B}$ and $1 \leq t \leq T$.

Following the same token in (4), the three constraints in (1), (2) and (5) can be replaced by the following single and equivalent constraint:

$$\sum_{i \in \mathcal{T}_j} x_{ij}^b(t) + \sum_{k \in \mathcal{T}_p} x_{pk}^b(t) \leq 1, \quad (6)$$

where $p \in \mathcal{I}_j, j \in \mathcal{N}, j \neq k, b \in \mathcal{B}$ and $1 \leq t \leq T$.

C. Traffic Modeling

1) *Flow Routing for Primary Sessions*: For flexibility and load balancing, we allow flow splitting in the network. That is, the flow rate of a session may split and merge inside the network \mathcal{N} in whatever loop-free manner as long as it can maximize the data rate $\hat{r}(l)$ of session $l \in \hat{\mathcal{L}}$. Denote $\hat{s}(l)$ and $\hat{d}(l)$ as the source and destination nodes of primary session $l \in \hat{\mathcal{L}}$, respectively. Denote $\hat{f}_{ij}(l)$ as the data rate on link (i, j) that is attributed to primary session $l \in \hat{\mathcal{L}}$, where $i \in \mathcal{N}$ and $j \in \mathcal{T}_i$. We have the following flow balance constraints:

- If node i is the source node of primary session $l \in \hat{\mathcal{L}}$ (i.e., $i = \hat{s}(l)$), then

$$\sum_{j \in \mathcal{T}_i} \hat{f}_{ij}(l) = \hat{r}(l) \quad (l \in \hat{\mathcal{L}}, i = \hat{s}(l)). \quad (7)$$

- If node i is an intermediate relay node for primary session l (i.e., $i \neq \hat{s}(l)$ and $i \neq \hat{d}(l)$), then

$$\sum_{j \in \mathcal{T}_i} \hat{f}_{ij}(l) = \sum_{k \in \mathcal{T}_i} \hat{f}_{ki}(l) \quad (l \in \hat{\mathcal{L}}, i \in \mathcal{N}). \quad (8)$$

- If node i is the destination node of primary session l (i.e., $i = \hat{d}(l)$), then

$$\sum_{k \in \mathcal{T}_i} \hat{f}_{ki}(l) = \hat{r}(l) \quad (l \in \hat{\mathcal{L}}, i = \hat{d}(l)). \quad (9)$$

It can be easily verified that once (7) and (8) are satisfied, then (9) is also satisfied. As a result, it is sufficient to list only (7) and (8) in the formulation.

2) *Flow Routing for Secondary Sessions*: Denote $s(m)$ and $d(m)$ as the source and destination nodes of secondary session $m \in \mathcal{L}$, respectively. Denote $f_{ij}(m)$ as the data rate on link (i, j) that is attributed to secondary session $m \in \mathcal{L}$. Similar to that for the primary sessions, we allow flow splitting for the secondary sessions. We have the following flow balance constraints:

- If node i is the source node of secondary session $m \in \mathcal{L}$ (i.e., $i = s(m)$), then we have

$$\sum_{j \in \mathcal{T}_i} f_{ij}(m) = r(m) \quad (m \in \mathcal{L}, i = s(m)). \quad (10)$$

- If node i is an intermediate relay node for secondary session m (i.e., $i \neq s(m)$ and $i \neq d(m)$), then

$$\sum_{j \in \mathcal{T}_i} f_{ij}(m) = \sum_{k \in \mathcal{T}_i} f_{ki}(m) \quad (m \in \mathcal{L}, i \in \mathcal{N}). \quad (11)$$

- If node i is the destination node of secondary session m (i.e., $i = d(m)$), then

$$\sum_{k \in \mathcal{T}_i} f_{ki}(m) = r(m) \quad (m \in \mathcal{L}, i = d(m)). \quad (12)$$

Again, to avoid redundancy, it is sufficient to list only (10) and (11) in the formulation.

3) *Link Capacity Constraints*: For each link (i, j) , denote the link capacity on channel b as C_{ij}^b , i.e., $C_{ij}^b = W_b \log_2 \left(1 + \frac{\rho_i d_{ij}^{-\gamma} \lambda}{N_0} \right)$, where W_b is the bandwidth for channel b , ρ_i is the power spectral density from transmit node i , d_{ij} is the distance between nodes i and j , γ is the path loss index, λ is the antenna related constant, and N_0 is the ambient Gaussian noise density. Since the aggregate flow rate from the primary and secondary sessions on each link (i, j) cannot exceed the average link rate (over T time slots), we have

$$\sum_{l \in \hat{\mathcal{L}}} \hat{f}_{ij}(l) + \sum_{m \in \mathcal{L}} f_{ij}(m) \leq \frac{1}{T} \sum_{t=1}^T \sum_{b \in \mathcal{B}} C_{ij}^b \cdot x_{ij}^b(t). \quad (13)$$

D. Multiobjective Formulation

Our goal is to find the optimal throughput curve for both the primary and secondary sessions. This problem can be formulated as a *multicriteria* optimization program with the objectives of maximizing session throughput in both primary and secondary networks. For throughput maximization, we maximize the minimum session rate in each network to ensure fairness. We define \hat{r}_{\min} and r_{\min} as the minimum rate among the primary and secondary sessions, respectively. Then we have:

$$\hat{r}_{\min} \leq \hat{r}(l) \quad (l \in \hat{\mathcal{L}}), \quad (14)$$

$$r_{\min} \leq r(m) \quad (m \in \mathcal{L}). \quad (15)$$

The multiobjective program can be written as follows:

BIOPT

$$\max \hat{r}_{\min}$$

$$\max r_{\min}$$

s.t. Self interference constraints : (4);

Mutual interference constraints : (6);

Flow routing for primary sessions : (7), (8);

Flow routing for secondary sessions : (10), (11);

Link capacity constraints : (13);

Minimum sessions rate constraints : (14), (15).

In this formulation, C_{ij}^b are constants, $x_{ij}^b(t)$ are binary variables, $\hat{f}_{ij}(l)$, $f_{ij}(m)$, $\hat{r}(l)$, \hat{r}_{\min} , $r(m)$ and r_{\min} are continuous variables. This formulation is in the form of *multiobjective mixed-integer linear programming* (MOMILP). In the next section, we develop an efficient algorithm to solve this problem.

III. AN APPROXIMATION ALGORITHM

A. Background and Roadmap

For optimization problem BIOPT, we want to maximize the minimum achievable throughput in both the primary and secondary networks. Since the two objective functions, \hat{r}_{\min} and r_{\min} , are conflicting with each other, we pursue *Pareto-optimal* solutions [4]. For ease of exposition, we define $\alpha = \{\mathbf{x}, \mathbf{f}, \hat{\mathbf{r}}, \mathbf{r}, \hat{r}_{\min}, r_{\min}\}$ as a feasible solution to BIOPT,

where $\mathbf{x}, \mathbf{f}, \hat{\mathbf{f}}, \mathbf{r}$, and $\hat{\mathbf{r}}$ represent the set of $x_{ij}, f_{ij}, \hat{f}_{ij}, r(m)$ and $\hat{r}(l)$ for $i \in \mathcal{X}, j \in \mathcal{X}, l \in \hat{\mathcal{L}}$ and $m \in \mathcal{L}$. For a feasible solution α , we denote $U(\alpha)$ and $V(\alpha)$ as

$$U(\alpha) = \hat{r}_{\min}, \quad (16)$$

$$V(\alpha) = r_{\min}. \quad (17)$$

Then BIOPT can be re-written as follows:

BIOPT

$$\max U(\alpha)$$

$$\max V(\alpha)$$

$$\text{s.t. } \alpha = \{\mathbf{x}, \mathbf{f}, \hat{\mathbf{f}}, \mathbf{r}, \hat{\mathbf{r}}, r_{\min}, \hat{r}_{\min}\};$$

$$\text{Constraints (4), (6)–(8), (10), (11), (13)–(17).}$$

For a Pareto-optimal solution α^\dagger , the corresponding objective pair (U^\dagger, V^\dagger) is called a *Pareto-optimal point*. For a Pareto-optimal point (U^\dagger, V^\dagger) , there does not exist another feasible solution α with objective pair (U, V) such that $U \geq U^\dagger$ and $V > V^\dagger$, or $U > U^\dagger$ and $V \geq V^\dagger$. This means that it is impossible to further improve any one objective without deteriorating the other. For our problem, it is difficulty to find Pareto-optimal point directly. Therefore, we find a *weakly Pareto-optimal point* first and then find the corresponding Pareto-optimal point. For a feasible solution α^* , with corresponding objective pair (U^*, V^*) , if there does not exist any other solution α with its objective pair (U, V) such that $U > U^*$ and $V > V^*$, then solution α^* is called a *weakly Pareto-optimal solution* and (U^*, V^*) is called a *weakly Pareto-optimal point*. From this definition, it is obvious that a Pareto-optimal point is also a weakly Pareto-optimal point, while a weakly Pareto-optimal point is not always Pareto optimal.

To find all the Pareto-optimal points for BIOPT, we can combine the two objectives into a single criterion. There are two main techniques to transform a multiobjective problem into a single-objective problem: (i) weighted sum method and (ii) Chebyshev norm method. In the weighed sum method, the objective is defined as a nonnegative linear combination of the two objective functions through a parameter $0 \leq \beta \leq 1$:

$$\max \beta \cdot U(\alpha) + (1 - \beta) \cdot V(\alpha). \quad (18)$$

Although it is easy to find a Pareto-optimal point for a given β , it is difficult to find *all* Pareto-optimal points using this method. This is because there is an infinite number of β values between $[0, 1]$ and it is impossible to check out all these values for Pareto-optimal points. So the weighted sum method is not a good choice to solve our problem.

In this paper, we employ the Chebyshev norm method, which allows us to find all Pareto-optimal points by identifying *specific* values of β (instead of enumerating all values blindly). The Chebyshev norm between two points A and B with (U_A, V_A) and (U_B, V_B) , respectively, is defined as follows:

$$\|A - B\| = \max\{|U_A - U_B|, |V_A - V_B|\}. \quad (19)$$

The *weighted* Chebyshev norm with weight $0 \leq \beta \leq 1$ is defined as follows:

$$\|A - B\|_\beta = \max\{\beta|U_A - U_B|, (1 - \beta)|V_A - V_B|\}. \quad (20)$$

In the rest of this section, we give the single-objective problem formulation from BIOPT via weighted Chebyshev norm. Then we show how to find new Pareto-optimal points by properly setting the value of β in each iteration. In the case when there is an infinite number of Pareto-optimal points, we show how to terminate the iteration when we have achieved ε -approximation in the objective value. Finally, by connecting all Pareto-optimal points that we found in the iterations, we obtain the throughput curve and prove that its approximation error to optimal is no more than ε .

B. Single Objective Formulation With Chebyshev Norm

To transform our multiobjective problem into a single objective problem, we define an ideal point I with coordinate (U_I, V_I) such that for any feasible solution α with $(U(\alpha), V(\alpha))$, we have $U(\alpha) \leq U_I$ and $V(\alpha) \leq V_I$. In other words, U_I is an upper bound of $U(\alpha)$ and V_I is an upper bound of $V(\alpha)$, respectively, for any α . Based on this ideal point I , we define weighted Chebyshev norm between a feasible solution point α with $(U(\alpha), V(\alpha))$ and (U_I, V_I) as $\max\{\beta|U_I - U(\alpha)|, (1 - \beta)|V_I - V(\alpha)|\}$. We are interested in the minimum value of weighted Chebyshev norm over all feasible solutions, i.e.,

$$\min_{\alpha} \max\{\beta(U_I - U(\alpha)), (1 - \beta)(V_I - V(\alpha))\}, \quad (21)$$

where the minimization is taken over all feasible solutions α for BIOPT, and $\beta \in [0, 1]$. We now show that for a given β , the optimal objective pair(s) $(U(\alpha), V(\alpha))$ (may not be unique) in (21) are weakly Pareto-optimal points.

Lemma 1: For any given $\beta \in [0, 1]$, the optimal objective pairs from (21) are weakly Pareto-optimal points.

The proof of Lemma 1 is given in Appendix 1. There is an infinite number of points that can be used as the ideal point. For simplicity, we choose our ideal point I with (U_I, V_I) as follows. For U_I , we set it to the maximum objective value of U when V is set to 0 in BIOPT. Likewise, for V_I , we set it to the maximum objective value of V when U is set to 0 in BIOPT. Then, we have a single objective formulation as follows:

$$\min \max \{\beta|U_I - U(\alpha)|, (1 - \beta)|V_I - V(\alpha)|\}$$

$$\text{s.t. } \alpha = \{\mathbf{x}, \mathbf{f}, \hat{\mathbf{f}}, \mathbf{r}, \hat{\mathbf{r}}, r_{\min}, \hat{r}_{\min}\};$$

$$\beta \in [0, 1];$$

$$\text{Constraints (4), (6)–(8), (10), (11), (13)–(17).}$$

Since the objective function in the above formulation is nonlinear, we define $z = \max\{\beta|U_I - U(\alpha)|, (1 - \beta)|V_I - V(\alpha)|\}$. Then we have:

BIOPT – L

$$\min z$$

$$\text{s.t. } z \geq \beta(U_I - U(\alpha));$$

$$z \geq (1 - \beta)(V_I - V(\alpha));$$

$$\alpha = \{\mathbf{x}, \mathbf{f}, \hat{\mathbf{f}}, \mathbf{r}, \hat{\mathbf{r}}, r_{\min}, \hat{r}_{\min}\};$$

$$\beta \in [0, 1];$$

$$\text{Constraints (4), (6)–(8), (10), (11), (13)–(17).}$$

Algorithm 1 Weakly Pareto to Pareto

1. *Input: Weakly Pareto-optimal point (U^*, V^*) ;*
2. *Solve BIOPT with the additional constant $V = V^*$ to obtain the optimal U^\dagger ;*
3. *Solve BIOPT with the additional constant $U = U^\dagger$ to obtain the optimal V^\dagger ;*
4. *Return (U^\dagger, V^\dagger) .*

Now, the objective function is linear. For a given β , BIOPT-L is in the form of mixed-integer linear program (MILP), which is NP-hard in general. But fortunately, all integer variables in this MILP are binary. For binary variables that can only take 0 and 1, a branch-and-cut based solution procedure used by a commercial solver such as CPLEX is very efficient. Therefore, we will use CPLEX to solve all our binary MILP problems, which turns out to be very successful for all practical purposes.

C. Finding Pareto-Optimal Point for a Given β

From Lemma 1, we know that for a given β , the optimal objective pair obtained from BIOPT-L is a weakly Pareto-optimal point. For this weakly Pareto-optimal point (U^*, V^*) , we can find the corresponding Pareto-optimal point (U^\dagger, V^\dagger) based on the Algorithm 1.

From line 2 in Algorithm 1, we know there does not exist another point (U, V) with $U > U^\dagger$ and $V \geq V^*$. From line 3, we know that $V^\dagger \geq V^*$, and there does not exist any other point with $U \geq U^\dagger$ and $V > V^\dagger$. Therefore, there does not exist any other point (U, V) with $U > U^\dagger$ and $V \geq V^\dagger$, or $U \geq U^\dagger$ and $V > V^\dagger$. Then (U^\dagger, V^\dagger) is a Pareto-optimal point. It is obvious that the weakly Pareto-optimal point (U^*, V^*) and the corresponding Pareto-optimal point (U^\dagger, V^\dagger) can achieve the same z for BIOPT-L. We omit its proof here to conserve space.

D. Determination of New Pareto-Optimal Points

In the last section, we showed that for a given β , we can find its corresponding Pareto-optimal point. Since there is an infinite number of values for β between $[0, 1]$ and different β values may correspond to the same Pareto-optimal point, it is important to identify a subset of β values to find all Pareto-optimal points. In this section, we propose a method to determine a β value based on two given Pareto-optimal points. This β value allows us to find a new Pareto-optimal point.

For any two given Pareto-optimal points A with (U_A, V_A) and B with (U_B, V_B) , suppose $U_A < U_B$ and $V_A > V_B$ in problem BIOPT-L. Define

$$\beta_{AB} = \frac{(V_I - V_B)}{(U_I - U_A + V_I - V_B)}. \quad (22)$$

Denote K as the point that corresponds to β_{AB} (by solving BIOPT-L and applying Algorithm 1). The point K has the following property.

Property 1: If there exists at least one Pareto-optimal point between A and B , then K is one such Pareto-optimal point; otherwise, K coincides with either A or B .

The proof of Property 1 is given in Appendix 2. The significance of Property 1 is that it allows us to find new Pareto-optimal points iteratively based on two known Pareto-optimal points. So we can start from two known Pareto-optimal points $\{Q_1, Q_2\}$. Based on these two points, we calculate β as in (22) to find new Pareto-optimal point Q_3 . We now have two intervals: $\{Q_1, Q_3\}$ and $\{Q_3, Q_2\}$. For each interval, we find its β and a new Pareto-optimal point. In the case when the Pareto-optimal point coincides with any of the two end points, we declare that there does not exist a new Pareto-optimal point in this interval. The process continues as long as we can find new Pareto-optimal point for some interval. When the total number of Pareto-optimal points is not large, our algorithm will terminate with all Pareto-optimal points. But when the number of Pareto-optimal points is very large (possibly infinite number of points), we need a way to terminate the iterations. In our algorithm, we set the following termination condition. For the interval between A and B , if

$$\max\{U_B - U_A, V_A - V_B\} \leq \varepsilon, \quad (23)$$

then we stop to find any new Pareto-optimal point in this interval. In the next section, we show that such a termination condition can guarantee a maximum throughput curve that is ε -approximate to the optimal curve.

For the β values defined by (22), we have the following result, which is a point of related interest with respect to the stability of solutions to BIOPT-L.

Property 2: Suppose $(U_1, V_1), (U_2, V_2), \dots, (U_M, V_M)$ are all Pareto-optimal points between Q_1 and Q_M with $U_1 < U_2 < \dots < U_M$, where M could go to infinite. Then, we have the following relationships for the corresponding $\beta_{(K-1)K}$:

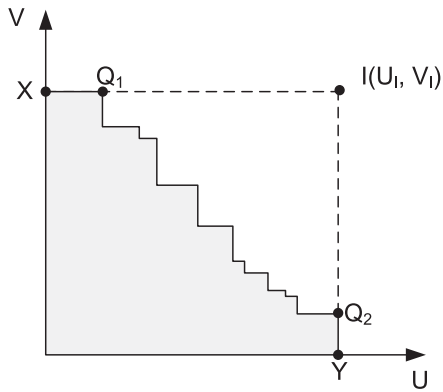
$$\beta_{12} < \beta_{23} < \dots < \beta_{(M-1)M}.$$

Moreover, for any $\beta \in (\beta_{(K-1)K}, \beta_{K(K+1)})$, we have that (U_K, V_K) is the corresponding Pareto-optimal point found via the BIOPT-L (note that by Property 1, for $\beta = \beta_{(K-1)K}$, we have that either (U_{K-1}, V_{K-1}) or (U_K, V_K) is optimal, for each $K = 2, \dots, M$).

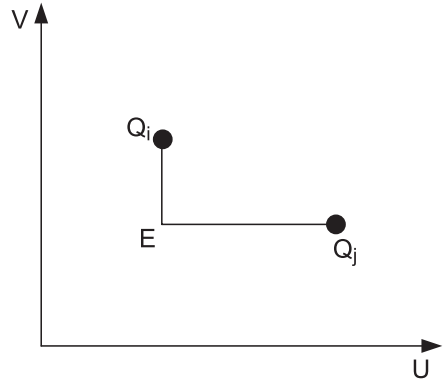
The proof of Property 2 is given in Appendix 3.

E. Main Result

We are now ready to describe the complete algorithm to find the necessary number of Pareto-optimal points that can be used to construct a throughput curve. As shown in Fig. 2(a), we start with our ideal point $I(U_I, V_I)$ and weakly Pareto-optimal points X and Y with $(0, V_I)$ and $(U_I, 0)$, respectively. By using Algorithm 1, we can find the Pareto-optimal points Q_1 and Q_2 corresponding to X and Y , respectively. Note that when X and Y are already Pareto-optimal, then Q_1 and Q_2 will coincide with X and Y , respectively. Starting from the interval with two end points Q_1 and Q_2 , we can find other new Pareto-optimal points iteratively. The iteration terminates when there is no new Pareto-optimal point for each interval or the interval is sufficiently small (as in (23)). Since there is a non-null continuous interval between any two neighboring Pareto-optimal points, the total



(a) The ideal point and two starting Pareto-optimal points.



(b) Throughput curve between any two consecutive Q_i and Q_j .

Fig. 2. Assuming K does not fall between A and B .

number of Pareto-optimal points in \mathcal{G} is thus finite. Based on the weakly Pareto-optimal points X and Y , and Pareto-optimal points Q_1, \dots, Q_2 that we have found in the iterations, we have a throughput curve as follows: i) connect X and Q_1 with a line, ii) make an “L”-shape connection between any two consecutive Pareto-optimal points between Q_i and Q_j as shown in Fig. 2(b), and iii) connect Q_2 and Y with a line. Fig. 3 summarizes our discussions.

Theorem 1: The throughput curve from Figure 3 approximates the optimal bicriteria throughput curve with the approximation error being no more than ε .

The proof of Theorem 1 is given in Appendix 4.

IV. A CASE STUDY

In this section, we perform a numerical study on a primary and secondary networks. Our goal is twofold. First, we want to demonstrate how our algorithm finds throughput curve for the bicriteria optimization problem. Second, we want to compare the throughput region (the area under the throughput curve) under the UPS policy to that under the interweave.

A. Simulation Setting

We consider a randomly generated 15-node primary network and 15-node secondary network in a 100×100 area. For generality, we normalize the units for distance, bandwidth, power and data rate with appropriate dimensions. The location

Plotting Throughput Curve

1. **Initialization:** Find ideal point I , weakly Pareto-optimal points X and Y , and corresponding Pareto-optimal points Q_1 and Q_2 ;
2. Set $\mathcal{Z} = \{\{Q_1, Q_2\}\}$, and $\mathcal{G} = \{Q_1, Q_2\}$;
3. while ($\mathcal{Z} \neq \emptyset$) {
4. Take an interval, say $\{Q_i, Q_j\}$, from set \mathcal{Z} ;
5. If ($\max\{U_{Q_j} - U_{Q_i}, V_{Q_i} - V_{Q_j}\} > \varepsilon$) {
6. Compute $\beta_{Q_i Q_j}$ based on (22) to find new Pareto-optimal point Q_k ;
7. If Q_k coincides with Q_i or Q_j , then Q_i and Q_j are two adjacent Pareto-optimal points;
8. Otherwise, Q_k is a new Pareto-optimal point; $\mathcal{Z} = \mathcal{Z} \cup \{\{Q_i, Q_k\}, \{Q_k, Q_j\}\}$, $\mathcal{G} = \mathcal{G} \cup \{Q_k\}$;
9. Remove $\{Q_i, Q_j\}$ from \mathcal{Z} ;
10. Draw throughput curve based on X , Y , and all Pareto-optimal points in \mathcal{G} .

Fig. 3. Pseudo-code of an approximation algorithm to find the proposed $(1 - \varepsilon)$ -optimal throughput curve.

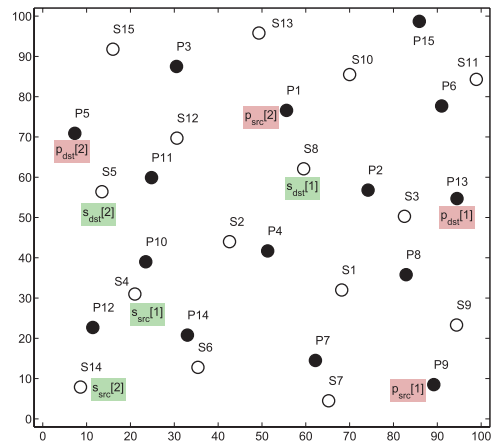


Fig. 4. The locations of a 15-node primary network and a 15-node secondary network.

of each node is shown in Fig. 4. We assume that there are two primary sessions in the primary network and two secondary sessions in the secondary network. The source and destination nodes for each session are randomly chosen in their networks and are also shown in Fig. 4.

We assume there are two channels in the primary network ($\mathcal{B} = \{1, 2\}$), with the bandwidth of each channel $b \in \mathcal{B}$ being $W_b = 10$. A time frame is divided into four time slots ($T = 4$). The transmission power spectral density ρ_i for each node $i \in \mathcal{N}$ is 1, the path loss index γ is 4, the antenna related constant λ is 1, and the ambient Gaussian noise density $N_0 = 10^{-6}$. We assume a node' transmission range and interference range are 30 and 50, respectively, in both primary and secondary networks. We set the approximation error for objective $\varepsilon = 0.1$.

B. Throughput Curve

For the above network setting, we apply our algorithm to BIOPT-L and find a sequence of Pareto-optimal points. We first set the ideal point I to (15.2235, 10.4497). Then we find two starting Pareto-optimal points Q_1 and Q_2 as (0, 10.4497) and (15.2235, 0), respectively. Based on these

TABLE II
NEW PARETO-OPTIMAL POINT THAT IS FOUND BY TWO KNOWN PARETO-OPTIMAL POINTS IN EACH ITERATION.
“PO” REPRESENTS PARETO-OPTIMAL POINTS

Iteration	Q_i	Q_j	$\beta_{Q_i Q_j}$	New PO point	Iteration	Q_i	Q_j	$\beta_{Q_i Q_j}$	New PO point
1	(0, 10.44)	(15.22, 0)	0.407	(10.5, 6.96)	36	(0.93, 9.33)	(1.0, 9.27)	—	—
2	(0, 10.44)	(10.5, 6.96)	0.186	(5.025, 8.11)	37	(1.0, 9.27)	(3.47, 9.26)	0.005	NO
3	(10.501, 6.96)	(15.223, 0)	0.688	(12.28, 4.53)	38	(4.20, 9.07)	(4.68, 8.45)	0.153	(4.6, 8.52)
4	(0, 10.44)	(5.02, 8.11)	0.133	(4.2, 9.07)	39	(4.68, 8.45)	(4.76, 8.36)	0.054	NO
5	(5.025, 8.11)	(10.5, 6.96)	0.254	(7.01, 8.0)	40	(8.46, 7.46)	(8.88, 7.45)	0.211	NO
6	(10.5, 6.96)	(12.289, 4.53)	0.556	(11.8, 6.00)	41	(8.88, 7.45)	(9.06, 7.27)	0.333	(9.0, 7.33)
7	(12.28, 4.53)	(15.22, 0)	0.780	(13.16, 3.55)	42	(9.06, 7.27)	(9.26, 7.07)	0.354	(9.19, 7.14)
8	(0, 10.44)	(4.206, 9.072)	0.082	(3.477, 9.26)	43	(9.26, 7.07)	(10.5, 6.96)	0.369	(9.33, 7.0)
9	(4.20, 9.07)	(5.025, 8.112)	0.175	(4.88, 8.25)	44	(0, 10.44)	(0.81, 9.45)	0.061	(0.76, 9.5)
10	(5.02, 8.11)	(7.01, 8.0)	0.193	(5.13, 8.02)	45	(0.81, 9.45)	(0.87, 9.4)	0.044	NO
11	(7.01, 8.0)	(10.50, 6.96)	0.298	(8.46, 7.46)	46	(4.2, 9.07)	(4.6, 8.52)	0.148	(4.54, 8.58)
12	(10.5, 6.96)	(11.8, 6.00)	0.485	NO	47	(4.6, 8.52)	(4.68, 8.45)	—	—
13	(11.8, 6.00)	(12.28, 4.53)	0.572	NO	48	(9.26, 7.07)	(9.33, 7.0)	—	—
14	(12.28, 4.53)	(13.16, 3.55)	0.702	NO	49	(9.33, 7.0)	(10.5, 6.96)	0.372	(9.36, 6.97)
15	(13.164, 3.554)	(15.223, 0)	0.835	NO	50	(0, 10.44)	(0.76, 9.5)	0.058	(0.72, 9.55)
16	(0, 10.44)	(3.47, 9.26)	0.072	(0.93, 9.33)	51	(0.76, 9.5)	(0.8, 9.45)	—	—
17	(3.47, 9.26)	(4.2, 9.07)	0.006	NO	52	(4.2, 9.07)	(4.54, 8.58)	0.144	(4.49, 8.63)
18	(4.2, 9.07)	(4.88, 8.25)	0.166	(4.76, 8.36)	53	(4.54, 8.58)	(4.6, 8.52)	—	—
19	(4.88, 8.25)	(5.02, 8.11)	0.184	(4.99, 8.13)	54	(9.33, 7.0)	(9.36, 6.97)	—	—
20	(5.02, 8.11)	(5.13, 8.02)	0.191	(5.16, 8.0)	55	(9.36, 6.97)	(10.5, 6.96)	0.272	NO
21	(5.13, 8.02)	(7.01, 8.0)	0.195	(5.16, 8.0)	56	(0, 10.44)	(0.72, 9.55)	0.055	(0.52, 9.58)
22	(7.01, 8.0)	(8.46, 7.46)	0.191	NO	57	(0.72, 9.55)	(0.76, 9.5)	—	—
23	(8.46, 7.46)	(10.5, 6.96)	0.340	(9.06, 7.27)	58	(4.2, 9.07)	(4.49, 8.63)	0.141	(4.45, 8.67)
24	(0, 10.44)	(0.93, 9.33)	0.068	(0.87, 9.4)	59	(4.49, 8.63)	(4.54, 8.58)	—	—
25	(0.93, 9.33)	(3.47, 9.26)	0.076	(1.0, 9.27)	60	(0, 10.44)	(0.52, 9.58)	0.036	NO
26	(4.2, 9.07)	(4.76, 8.36)	0.158	(4.68, 8.45)	61	(0.52, 9.58)	(0.72, 9.55)	0.037	NO
27	(4.76, 8.36)	(4.88, 8.25)	0.173	(4.86, 8.27)	62	(4.2, 9.07)	(4.45, 8.67)	0.138	(4.42, 8.71)
28	(4.88, 8.25)	(4.99, 8.13)	0.182	(4.97, 8.15)	63	(4.45, 8.67)	(4.49, 8.63)	—	—
29	(4.99, 8.13)	(5.02, 8.11)	—	—	64	(4.2, 9.07)	(4.42, 8.71)	0.136	(4.39, 8.74)
30	(5.13, 8.02)	(5.16, 8.0)	—	—	65	(4.42, 8.71)	(4.45, 8.67)	—	—
31	(5.16, 8.0)	(7.01, 8.0)	0.135	NO	66	(4.2, 9.07)	(4.39, 8.74)	0.086	NO
32	(8.46, 7.46)	(9.06, 7.27)	0.319	(8.88, 7.45)	67	(4.39, 8.74)	(4.42, 8.71)	—	—
33	(9.06, 7.27)	(10.5, 6.96)	0.361	(9.26, 7.07)					
34	(0, 10.44)	(0.87, 9.4)	0.064	(0.81, 9.45)					
35	(0.87, 9.4)	(0.93, 9.33)	—	—					

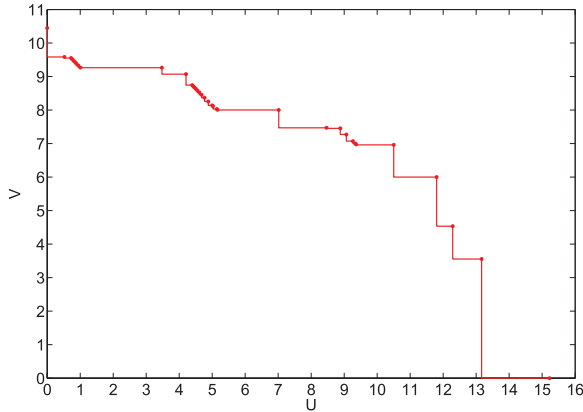


Fig. 5. The throughput curve found by our algorithm.

two starting Pareto-optimal points, Table II shows the results from our iterations. For each iteration, we have two Pareto-optimal points Q_i and Q_j . Based on these two points, we find $\beta_{Q_i Q_j}$ and the corresponding new Pareto-optimal point. In iteration 12–15, 17, 22, 31, 37, 39, 40, 45, 55, 60, 61, and 66, there does not exist a new Pareto-optimal point for the corresponding interval. In iteration 29, 30, 35, 36, 47, 48, 51, 53, 54, 57, 59, 63, 65, and 67, we stop finding Pareto-optimal points since the corresponding intervals between Q_i and Q_j are smaller than ε .

Based on the Pareto-optimal points in Table II, we plot the throughput curve as shown in Fig. 5. On this curve, the intervals corresponding to iterations 29, 30, 35, 36, 47, 48,

51, 53, 54, 57, 59, 63, 65, and 67 have ε -approximation to the optimal. For intervals corresponding to iterations 12–15, 17, 22, 31, 37, 39, 40, 45, 55, 60, 61 and 66, the throughput curve is optimal. These can be validated by choosing any point (U^*, V^*) on this curve and compare it with the corresponding optimal point. This optimal point can be obtained by solving BIOPT by setting the primary network throughput $U = U^*$. Then, we compare the maximum secondary network throughput value V with that we found from the curve. We first validate the points that locate within the intervals that achieve the ε -approximation. We set the primary network throughput $U^* = 4.65$, and solve BIOPT. The maximum secondary network throughput is $V = 8.476$. Based on the curve in Fig. 5, we can find the secondary network throughput $V^* = 8.457$. The difference between $V = 8.476$ and $V^* = 8.457$ is 0.019, which is smaller than $\varepsilon = 0.1$. For any point located in the intervals corresponding to iterations 29, 30, 35, 36, 47, 48, 51, 53, 54, 57, 59, 63, 65, and 67, we can obtain similar results. Next, we validate the results that are located in the intervals corresponding to iterations 12–15, 17, 22, 31, 37, 39, 40, 45, 55, 60, 61 and 66. We choose the primary network throughput $U^* = 2.0$, and solve BIOPT by setting $U = U^*$. The obtained maximum secondary network throughput is $V = 9.270$. Based on the curve in Fig. 5, we can find the maximum secondary network throughput $V^* = 9.270$, which is the same as the optimal and the difference is smaller than ε . We can repeat the validation for any point located in intervals corresponding to iterations 12–15, 17, 22, 31, 37, 39,

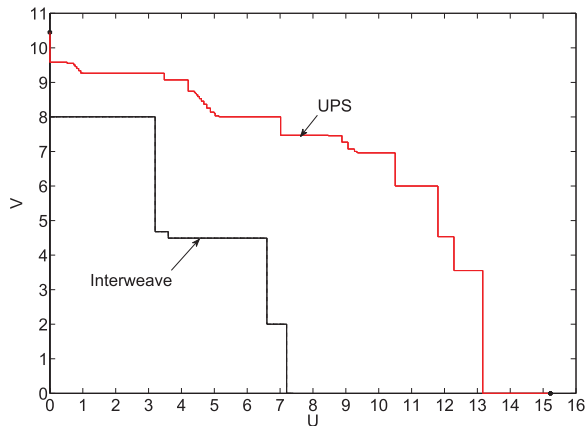


Fig. 6. A comparison of the throughput region under the UPS policy and the interweave paradigm.

40, 45, 55, 60, 61 and 66, and obtain the same conclusion. We omit showing these results here to conserve space.

Not shown in Table II are the feasible solutions for the Pareto-optimal points. In particular, in iterations 1–11, 16, 18–21, 23–28, 32–34, 38, 41–44, 46, 49, 50, 52, 56, 58, 62, and 64, we have found a Pareto-optimal solution α^\dagger when we solve the new Pareto-optimal point (U^\dagger, V^\dagger) . We now show how to find a feasible solution for *any* point on the throughput curve in Fig. 5.

Consider a point $(10, 6.96)$ on the throughput curve in Fig. 5. This point falls in the interval in iteration 55. Since this point is not a Pareto-optimal point, we do not know its feasible solution $\alpha^* = \{\mathbf{x}^*, \mathbf{f}^*, \hat{\mathbf{f}}^*, \mathbf{r}^*, \hat{\mathbf{r}}^*, \mathbf{r}_{\min}^*, \hat{\mathbf{r}}_{\min}^*\}$. We show how to construct a feasible solution for point $(10, 6.96)$ based on the solution for its corresponding Pareto-optimal point $(10.501, 6.96)$. For $(10.501, 6.96)$, denote its solution as $\alpha^\dagger = \{\mathbf{x}^\dagger, \mathbf{f}^\dagger, \hat{\mathbf{f}}^\dagger, \mathbf{r}^\dagger, \hat{\mathbf{r}}^\dagger, \mathbf{r}_{\min}^\dagger, \hat{\mathbf{r}}_{\min}^\dagger\}$. For α^* , we can use the same scheduling as in α^\dagger for both primary and secondary sessions, i.e., $\mathbf{x}^* = \mathbf{x}^\dagger$. For flow routing and data rate, there is no change for the secondary session, i.e., $\mathbf{f}^* = \mathbf{f}^\dagger$ and $\mathbf{r}^* = \mathbf{r}^\dagger$. But for the primary sessions, their throughput need to be adjusted, although their routing topology do not change. Specifically, we adjust the primary session throughput from 10.501 in α^\dagger to 10 in α^* , which will affect data rate on each link $\hat{\mathbf{f}}^*$. Therefore, we obtain a feasible solution α^* for point $(10, 6.96)$. For any point on this curve, we can use this method to construct one feasible solution based on the solution of its corresponding Pareto-optimal point.

C. Comparison With Other Paradigms

We now compare the UPS's throughput region (the area under the throughput curve) with other paradigms (i.e., underlay and interweave). Since the underlay paradigm requires interference cancellation capabilities (e.g, MIMO [20], [24], [25]) at the physical layer that is beyond what we have assumed for each node for UPS, it is not appropriate (or fair) to make such a comparison. So we will limit our comparison of UPS to the interweave paradigm [7]. Under interweave, the primary nodes use its network and spectrum resource without considerations of the secondary nodes. The secondary nodes

are allowed to use a spectrum band only when the primary nodes are not using it. There is no node-level cooperation between the two networks. Fig. 6 shows the throughput curves under the UPS and interweave paradigms. The throughput region (in terms of its area size) for the UPS policy is 2.64 times of that for the interweave. We also run 100 instances with different network settings to find the throughput curves between primary and secondary networks with our algorithm. The results are consistent and show that the throughput regions for the UPS policy are always much larger than those under the interweave paradigm.

V. CONCLUSIONS

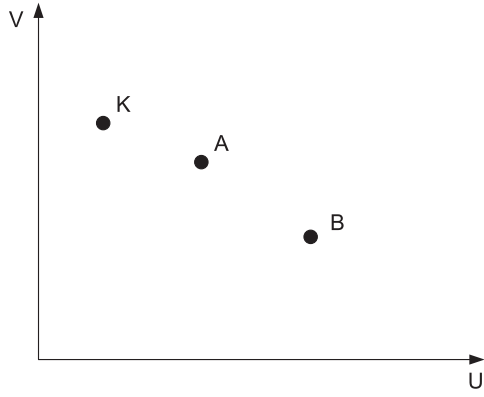
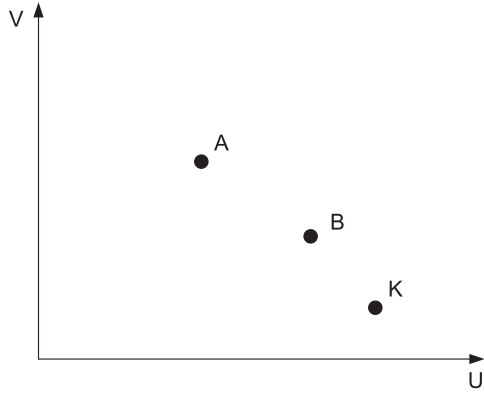
Node-level (data plane) cooperation between the primary and secondary networks adds a new dimension for efficient spectrum sharing. In this paper, we investigated achievable throughput region when the primary and secondary nodes are allowed to cooperate and forward each other's traffic. The achievable throughput region is characterized by the so-called optimal throughput curve. To find the optimal throughput curve, we formulated a multicriteria optimization problem and developed a novel solution based on weighted Chebyshev norm. Our solution is able to find a sequence of new Pareto-optimal points through iterations. We further showed that our throughput curve is an ε -approximation to the optimal curve. Through a case study, we showed that the throughput region under the UPS policy (with node-level cooperation) is substantially larger than that under the interweave paradigm (where there is no node-level cooperation).

APPENDIX 1 PROOF OF LEMMA 1

Proof: This proof is based on contradiction. For a given β , suppose that the optimal objective pairs H with (U_H, V_H) achieves the minimum Chebyshev norm for (21), but H is not a weakly Pareto-optimal point. Then, there must exists another point K with objective pair (U_K, V_K) , that has $U_K > U_H$ and $V_K > V_H$. The weighted Chebyshev norms between H and I , K and I are $\max\{\beta(U_I - U_H), (1 - \beta)(V_I - V_H)\}$ and $\max\{\beta(U_I - U_K), (1 - \beta)(V_I - V_K)\}$, respectively. Since $(U_I - U_K) < (U_I - U_H)$ and $(V_I - V_K) < (V_I - V_H)$, we have $\beta(U_I - U_K) < \beta(U_I - U_H)$ and $(1 - \beta)(V_I - V_K) < (1 - \beta)(V_I - V_H)$. Therefore, $\max\{\beta(U_I - U_K), (1 - \beta)(V_I - V_K)\} < \max\{\beta(U_I - U_H), (1 - \beta)(V_I - V_H)\}$. This means K can achieve a smaller Chebyshev norm than H , which contradicts with the assumption that (U_H, V_H) can achieve the minimum Chebyshev norm. Therefore, for any given $\beta \in [0, 1]$, the optimal objective pair H that achieves the minimum chebyshev norm for (21) is always weakly Pareto-optimal point. ■

APPENDIX 2 PROOF OF PROPERTY 1

Proof: Our proof consists of three steps. We first show that K falls between A and B . Next, we show that if there exists other Pareto-optimal points between A and B , then K falls strictly between A and B . Finally, we show that if no

(a) The point K falls to the left of A .(b) The point K falls to the right of B .Fig. 7. Assuming K does not fall between A and B .

other Pareto-optimal points exist between A and B , then K coincides with either A or B .

Step 1: We first show that K falls between A and B . Our proof is based on the contradiction by assuming: (i) K falls to the left of A ; (ii) K falls to the right of B .

- (i) In this case, we assume K falls to the left of A (see Fig. 7(a)). For any Pareto-optimal point (U^\dagger, V^\dagger) that is between A and B , we have $U_K < U^\dagger$ and $V_K > V^\dagger$. The objective value z_K with respect to (U_K, V_K) has the following constraints:

$$z_K \geq \beta_{AB}(U_I - U_K), \quad z_K \geq (1 - \beta_{AB})(V_I - V_K)$$

with at least one constraint satisfying the equality. For point (U^\dagger, V^\dagger) , its objective value z^\dagger has the following constraints:

$$z^\dagger \geq \beta_{AB}(U_I - U^\dagger), \quad z^\dagger \geq (1 - \beta_{AB})(V_I - V^\dagger)$$

with at least one constraint satisfying the equality. Since $U_K < U^\dagger$ and $V_K > V^\dagger$, then we have $\beta_{AB}(U_I - U_K) > \beta_{AB}(U_I - U^\dagger)$ and $(1 - \beta_{AB})(V_I - V_K) < (1 - \beta_{AB})(V_I - V^\dagger)$. In order to find the relationships between z_K and z^\dagger , we discuss two cases:

- If $\beta_{AB}(U_I - U^\dagger) \geq (1 - \beta_{AB})(V_I - V^\dagger)$, then $z^\dagger = \beta_{AB}(U_I - U^\dagger)$. Since $z_K \geq \beta_{AB}(U_I - U_K) > \beta_{AB}(U_I - U^\dagger)$, then $z_K > z^\dagger$.

- If $\beta_{AB}(U_I - U^\dagger) < (1 - \beta_{AB})(V_I - V^\dagger)$, then $z^\dagger = (1 - \beta_{AB})(V_I - V^\dagger)$. Since $\beta_{AB}(U_I - U_K) > \beta_{AB}(U_I - U^\dagger)$ is known, we compare $\beta_{AB}(U_I - U_K)$ with $(1 - \beta_{AB})(V_I - V^\dagger)$. Since $U_K < U_A$, then

$$\begin{aligned} \beta_{AB}(U_I - U_K) &> \beta_{AB}(U_I - U_A) \\ &= \frac{V_I - V_B}{U_I - U_A + V_I - V_B}(U_I - U_A). \end{aligned}$$

Since $V^\dagger > V_B$, then

$$\begin{aligned} (1 - \beta_{AB})(V_I - V^\dagger) &< (1 - \beta_{AB})(V_I - V_B) \\ &= \frac{U_I - U_A}{U_I - U_A + V_I - V_B}(V_I - V_B). \end{aligned}$$

Therefore, $z_K \geq \beta_{AB}(U_I - U_K) > (1 - \beta_{AB})(V_I - V^\dagger) = z^\dagger$.

Based on the above discussion, we find that $z_K > z^\dagger$, which means that any Pareto-optimal point between A and B can achieve a smaller z than K . This contradicts that K can achieve the minimum z (minimum Chebyshev norm) for BIOPT-L. Therefore, K can not fall to the left of A .

- (ii) The discussion for the case that K cannot fall to the right of B (Fig. 7(b)) is similar to case (i), we omit it here to conserve space.

From (i) and (ii), we conclude that the Pareto-optimal point K found by setting β_{AB} as in (22) falls between A and B .

Step 2: From Step 1, we showed that K falls between A and B . Here, we show that if there exists new Pareto-optimal points between A and B , then the Pareto-optimal point K found by β_{AB} will be a new point different from A and B . To show this, we only need to show that all Pareto-optimal points that fall strictly between A and B can achieve a smaller z than A and B .

For any Pareto-optimal point with (U^\dagger, V^\dagger) that falls strictly between A and B , we have $U_A < U^\dagger < U_B$ and $V_A > V^\dagger > V_B$. We define z^\dagger, z_A, z_B as the objective values for BIOPT-L corresponding to Pareto-optimal points (U^\dagger, V^\dagger) , A and B , respectively. Therefore, we have:

$$\begin{aligned} z^\dagger &\geq \beta_{AB}(U_I - U^\dagger), \quad z^\dagger \geq (1 - \beta_{AB})(V_I - V^\dagger); \\ z_A &\geq \beta_{AB}(U_I - U_A), \quad z_A \geq (1 - \beta_{AB})(V_I - V_A); \\ z_B &\geq \beta_{AB}(U_I - U_B), \quad z_B \geq (1 - \beta_{AB})(V_I - V_B). \end{aligned}$$

We now show that $z^\dagger < z_A$. We consider the different cases for the relationships between $\beta_{AB}(U_I - U^\dagger)$ and $(1 - \beta_{AB})(V_I - V^\dagger)$:

- If $\beta_{AB}(U_I - U^\dagger) \geq (1 - \beta_{AB})(V_I - V^\dagger)$, then $z^\dagger = \beta_{AB}(U_I - U^\dagger)$. Since $U_A < U^\dagger$, we have $\beta_{AB}(U_I - U_A) > \beta_{AB}(U_I - U^\dagger)$. Therefore, $z_A \geq \beta_{AB}(U_I - U_A) > \beta_{AB}(U_I - U^\dagger) = z^\dagger$.
- If $\beta_{AB}(U_I - U^\dagger) < (1 - \beta_{AB})(V_I - V^\dagger)$: then $z^\dagger = (1 - \beta_{AB})(V_I - V^\dagger)$. Since $U_A < U^\dagger$, we have $\beta_{AB}(U_I - U_A) > \beta_{AB}(U_I - U^\dagger)$. Now we compare $\beta_{AB}(U_I - U_A)$ with $(1 - \beta_{AB})(V_I - V^\dagger)$. Since $V^\dagger > V_B$, then $(1 - \beta_{AB})(V_I - V^\dagger) < (1 - \beta_{AB})(V_I - V_B) = \frac{(U_I - U_A)}{(U_I - U_A + V_I - V_B)}(V_I - V_B) = \beta_{AB}(U_I - U_A)$. Therefore, $z^\dagger < z_A$.

The proof for $z^\dagger < z_B$ is similar, and we omit it here.

From the above discussion, we find that any Pareto-optimal point (U^\dagger, V^\dagger) that falls strictly between A and B can achieve a smaller z than A and B . Therefore, the new Pareto-optimal point K (corresponding to β_{AB} in (22)) will fall strictly between A and B .

Step 3: We show that if there does not exist any new Pareto-optimal point between Pareto-optimal points A and B , then the Pareto-optimal point K will coincide with either A or B . In Section III-C, we showed that we can find a Pareto-optimal point for β_{AB} . From the above, we have shown that this Pareto-optimal point falls in the interval of A and B . If there is no other Pareto-optimal point between A and B , then the Pareto-optimal point K found by β_{AB} can only be either A or B . ■

APPENDIX 3 PROOF OF PROPERTY 2

Proof: (1). We first prove that $\beta_{12} < \beta_{23} < \dots < \beta_{(M-1)M}$.

Based on (22), we know $\beta_{(K-1)K} = \frac{V_I - V_K}{U_I - U_{K-1} + V_I - V_K}$ and $\beta_{K(K+1)} = \frac{V_I - V_{K+1}}{U_I - U_K + V_I - V_{K+1}}$. Then, they can also be expressed as follows:

$$\beta_{(K-1)K} = \frac{1}{\frac{U_I - U_{K-1}}{V_I - V_K} + 1} \quad \text{and} \quad \beta_{K(K+1)} = \frac{1}{\frac{U_I - U_K}{V_I - V_{K+1}} + 1}.$$

Since $U_{K-1} < U_i < U_{K+1}$ and $V_{K-1} > V_K > V_{K+1}$, then $\frac{U_I - U_{K-1}}{V_I - V_K} > \frac{U_I - U_K}{V_I - V_{K+1}}$, and so we can conclude that $\beta_{(K-1)K} = \frac{1}{\frac{U_I - U_{K-1}}{V_I - V_K} + 1} < \frac{1}{\frac{U_I - U_K}{V_I - V_{K+1}} + 1} = \beta_{K(K+1)}$.

Since $\beta_{(K-1)K} < \beta_{K(K+1)}$ for any adjacent Pareto-optimal points, we have

$$\beta_{12} < \beta_{23} < \dots < \beta_{(M-1)M}.$$

(2). We next prove that for any β where $\beta_{(K-1)K} < \beta < \beta_{K(K+1)}$, the corresponding Pareto-optimal point is (U_K, V_K) , i.e., (U_K, V_K) achieves the minimum z value.

For (U_K, V_K) , the objective value for BIOPT-L is z_K . For any other Pareto-optimal point (U_R, V_R) , we define its objective value as z_R . For z_K , we have

$$z_K \geq \beta(U_I - U_K), \quad z_K \geq (1 - \beta)(V_I - V_K).$$

If $\beta(U_I - U_K) \geq (1 - \beta)(V_I - V_K)$, then $z_K = \beta(U_I - U_K)$.

For (U_R, V_R) , we consider two cases:

- (i) If $U_R < U_K$ and $V_R > V_K$, then $z_K = \beta(U_I - U_K) < \beta(U_I - U_R) \leq z_R$.
- (ii) If $U_R > U_K$ and $V_R < V_K$, since $\beta < \beta_{K(K+1)}$, then we have

$$\begin{aligned} z_K &= \beta(U_I - U_K) < \beta_{K(K+1)}(U_I - U_K) \\ &= \frac{(V_I - V_{K+1})(U_I - U_K)}{U_I - U_K + V_I - V_{K+1}}, \\ z_R &= (1 - \beta)(V_I - V_R) > (1 - \beta_{K(K+1)})(V_I - V_R) \\ &= \frac{(U_I - U_K)(V_I - V_{K+1})}{U_I - U_K + V_I - V_{K+1}}. \end{aligned}$$

Therefore, $z_K < z_R$.

If $\beta(U_I - U_K) \leq (1 - \beta)(V_I - V_K)$, then $z_K = (1 - \beta)(V_I - V_K)$.

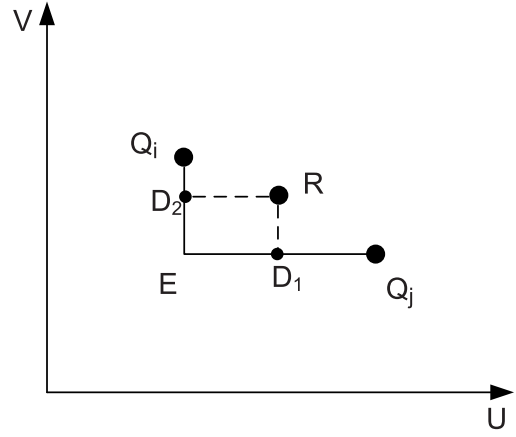


Fig. 8. The Pareto-optimal point R is represented by D_1 (or D_2) with an ε -approximation.

We also consider two cases for (U_R, V_R) :

- (i) $U_R > U_K$ and $V_R < V_K$: Thus $z_K = (1 - \beta)(V_I - V_K) < (1 - \beta)(V_I - V_R) \leq z_R$.
- (ii) $U_R < U_K$ and $V_R > V_K$: Since $\beta > \beta_{(K-1)K}$, then we have:

$$\begin{aligned} z_K &= (1 - \beta)(V_I - V_K) < (1 - \beta_{(K-1)K})(V_I - V_K) \\ &= \frac{(U_I - U_{K-1})(V_I - V_K)}{U_I - U_{K-1} + V_I - V_K}, \\ z_R &\geq \beta(U_I - U_R) > \beta_{(K-1)K}(U_I - U_R) \\ &= \frac{(V_I - V_K)(U_I - U_R)}{U_I - U_{K-1} + V_I - V_K}. \end{aligned}$$

Therefore, $z_K < z_R$, which is also a contradiction that z_R is the optimal solution.

Hence, for any Pareto-optimal point R , we have $z_K < z_R$, which implies that (U_K, V_K) is the optimal solution of BIOPT-L for $\beta \in (\beta_{(K-1)K}, \beta_{K(K+1)})$. ■

APPENDIX 4 PROOF OF THEOREM 1

Proof: We consider any two adjacent points Q_i and Q_j (see Fig. 8).

- If there does not exist any other Pareto-optimal points between Q_i and Q_j , then the curve $Q_i - E - Q_j$ is exactly the optimal throughput curve, since all points on this curve are weakly Pareto-optimal points.
- If there exist Pareto-optimal points between Q_i and Q_j , for any one of these Pareto-optimal points, say R with (U_R, V_R) , we have $U_{Q_i} < U_R < U_{Q_j}$ and $V_{Q_j} < V_R < V_{Q_i}$. When we use D_1 with (U_R, V_{Q_j}) (or D_2 with (U_{Q_i}, V_R)) to approximate R , then we have $\max\{U_R - U_{Q_i}, V_R - V_{Q_j}\} < \max\{U_{Q_j} - U_{Q_i}, V_{Q_i} - V_{Q_j}\} \leq \varepsilon$. Then, the approximation error by using D_1 (or D_2) to approximate R will be no more than ε .

Therefore, when we use $Q_i - E - Q_j$ to approximate the Pareto-optimal curve between Q_i and Q_j , the approximation error will be no more than ε . ■

ACKNOWLEDGMENTS

Part of W. Lou's work was completed while she was serving as a Program Director at the NSF. Any opinion, findings, and conclusions or recommendations expressed in this paper are those of the authors and do not reflect the views of the NSF. The authors thank Virginia Tech Advanced Research Computing for giving them access to the BlueRidge computer cluster.

REFERENCES

- [1] I. F. Akyildiz, W.-Y. Lee, M. C. Vuran, and S. Mohanty, "Next generation/dynamic spectrum access/cognitive radio wireless networks: A survey," *Comput. Netw.*, vol. 50, no. 13, pp. 2127–2159, Sep. 2006.
- [2] O. Bakr, M. Johnson, R. Mudumbai, and K. Ramchandran, "Multi-antenna interference cancellation techniques for cognitive radio applications," in *Proc. IEEE WCNC*, Budapest, Hungary, Apr. 2009, pp. 1–6.
- [3] P. K. Eswaran, A. Ravindran, and H. Moskowitz, "Algorithms for nonlinear integer bicriterion problems," *J. Optim. Theory Appl.*, vol. 63, no. 2, pp. 261–279, Nov. 1989.
- [4] M. Ehrgott, *Multicriterion Optimization*. New York, NY, USA: Springer-Verlag, 2005.
- [5] F. Gao, R. Zhang, Y.-C. Liang, and X. Wang, "Design of learning-based MIMO cognitive radio systems," *IEEE Trans. Veh. Technol.*, vol. 59, no. 4, pp. 1707–1720, May 2010.
- [6] S. Geirhofer, L. Tong, and B. M. Sadler, "Dynamic spectrum access in the time domain: Modeling and exploiting white space," *IEEE Commun. Mag.*, vol. 45, no. 5, pp. 66–72, May 2007.
- [7] A. Goldsmith, S. A. Jafar, I. Maric, and S. Srinivasa, "Breaking spectrum gridlock with cognitive radios: An information theoretic perspective," *Proc. IEEE*, vol. 97, no. 5, pp. 894–914, Apr. 2009.
- [8] S. Hua, H. Liu, M. Wu, and S. S. Panwar, "Exploiting MIMO antennas in cooperative cognitive radio networks," in *Proc. IEEE INFOCOM*, Shanghai, China, April. 2011, pp. 2714–2722.
- [9] S. K. Jayaweera, M. Bkassiny, and K. A. Avery, "Asymmetric cooperative communications based spectrum leasing via auctions in cognitive radio networks," *IEEE Trans. Wireless Commun.*, vol. 10, no. 8, pp. 2716–2724, Aug. 2011.
- [10] S.-J. Kim and G. B. Giannakis, "Optimal resource allocation for MIMO ad hoc cognitive radio networks," *IEEE Trans. Inf. Theory*, vol. 57, no. 5, pp. 3117–3131, May 2011.
- [11] R. Manna, R. H. Louie, Y. Li, and B. Vucetic, "Cooperative spectrum sharing in cognitive radio networks with multiple antennas," *IEEE Trans. Signal Process.*, vol. 59, no. 11, pp. 5509–5522, Nov. 2011.
- [12] T. Nadkar, V. Thumar, G. Shenoy, A. Mehta, U. B. Desai, and S. N. Merchant, "A cross-layer framework for symbiotic relaying in cognitive radio networks," in *Proc. IEEE DySPAN*, Aachen, Germany, May 2011, pp. 498–509.
- [13] President's Council of Advisors on Science and Technology (PCAST). (Jul. 2012). *Report to the President—Realizing the Full Potential of Government-Held Spectrum to Spur Economic Growth*. [Online]. Available: http://www.whitehouse.gov/sites/default/files/microsites/ostp/pcast_spectrum_report_final_july_20_2012.pdf
- [14] T. K. Ralphs, M. J. Saltzman, and M. M. Wiecek, "An improved algorithm for solving biobjective integer programs," *Ann. Oper. Res.*, vol. 147, no. 1, pp. 43–70, Oct. 2006.
- [15] O. Simeone, I. Stanojev, S. Savazzi, Y. Bar-Ness, U. Spagnolini, and R. Pickholtz, "Spectrum leasing to cooperating secondary ad hoc networks," *IEEE J. Sel. Areas Commun.*, vol. 26, no. 1, pp. 203–213, Jan. 2008.
- [16] R. E. Steuer and E.-U. Choo, "An interactive weighted tchebycheff procedure for multiple objective programming," *Math. Program.*, vol. 26, no. 3, pp. 326–344, Oct. 1983.
- [17] W. Su, J. D. Matyjas, and S. Batalama, "Active cooperation between primary users and cognitive radio users in cognitive ad-hoc networks," in *Proc. IEEE ICASSP*, Mar. 2010, pp. 3174–3177.
- [18] A. M. Wyglinski, M. Nekovee, and Y. T. Hou, *Cognitive Radio Communications and Networks: Principles and Practice*. San Diego, CA, USA: Academic, 2010.
- [19] X. Yuan, Y. Shi, Y. T. Hou, W. Lou, and S. Kompella, "UPS: A united cooperative paradigm for primary and secondary networks," in *Proc. IEEE MASS*, Hangzhou, China, Oct. 2013, pp. 78–85.
- [20] X. Yuan, C. Jiang, Y. Shi, Y. T. Hou, W. Lou, S. Kompella, and S. F. Midkiff, "Toward transparent coexistence for multihop secondary cognitive radio networks," *IEEE J. Sel. Areas Commun.*, vol. 33, no. 5, pp. 958–971, May 2015.
- [21] X. Yuan, F. Tian, Y. T. Hou, W. Lou, H. D. Sherali, S. Kompella, and J. H. Reed, "Optimal throughput curve for primary and secondary users with node-level cooperation," in *Proc. IEEE DySPAN*, Stockholm, Sweden, Sep./Oct. 2015, pp. 358–364.
- [22] J. Zhang and Q. Zhang, "Stackelberg game for utility-based cooperative cognitiveradio networks," in *Proc. ACM MobiHoc*, New Orleans, LA, USA, May 2009, pp. 23–32.
- [23] Q. Zhao and B. M. Sadler, "A survey of dynamic spectrum access," *IEEE Signal Process. Mag.*, vol. 24, no. 3, pp. 79–89, May 2007.
- [24] R. Zhang and Y.-C. Liang, "Exploiting multi-antennas for opportunistic spectrum sharing in cognitive radio networks," *IEEE J. Sel. Topics Signal Process.*, vol. 2, no. 1, pp. 88–102, Feb. 2008.
- [25] Y. J. A. Zhang and A. M.-C. So, "Optimal spectrum sharing in MIMO cognitive radio networks via semidefinite programming," *IEEE J. Sel. Areas Commun.*, vol. 29, no. 2, pp. 362–373, Feb. 2011.



Xu Yuan (S'13–M'16) received the Ph.D. degree from the Bradley Department of Electrical and Computer Engineering, Virginia Polytechnic Institute and State University, Blacksburg, VA, USA, in 2016. He is currently a Post-Doctoral Fellow of Electrical and Computer Engineering with the University of Toronto, Toronto, ON, Canada. His current research interests include algorithm design and optimization for spectrum sharing, coexistence, and cognitive radio networks.



Feng Tian (M'13) received the Ph.D. degree in signal and information processing from the Nanjing University of Posts and Telecommunications, Nanjing, China, in 2008, where he is currently an Associate Professor. He was a Visiting Scholar with Virginia Polytechnic Institute and State University, Blacksburg, VA, USA, from 2013 to 2015. His current research focuses on performance optimization and algorithm design for wireless networks.



Y. Thomas Hou (F'14) received the Ph.D. degree from the New York University Tandon School of Engineering (formerly Polytechnic University). He is currently a Bradley Distinguished Professor of Electrical and Computer Engineering with Virginia Polytechnic Institute and State University, Blacksburg, VA, USA. He has authored two graduate textbooks entitled *Applied Optimization Methods for Wireless Networks* (Cambridge University Press, 2014) and *Cognitive Radio Communications and Networks: Principles and Practices* (Academic Press/Elsevier, 2009). His current research focuses on developing innovative solutions to complex cross-layer optimization problems in wireless networks. He is the Steering Committee Chair of IEEE INFOCOM conference and a member of the IEEE Communications Society Board of Governors.



Wenjing Lou (F'15) received the Ph.D. degree in electrical and computer engineering from the University of Florida. She has been serving as a Program Director with the National Science Foundation, since 2014. She is currently a Professor with the Computer Science Department, Virginia Polytechnic Institute and State University. Her research interests are in the broad area of wireless networks, with special emphases on wireless security and cross-layer network optimization. She is the Steering Committee Chair of IEEE Conference on Communications and

Network Security.



Hanif D. Sherali is currently a University Distinguished Professor Emeritus with the Industrial and Systems Engineering Department, Virginia Polytechnic Institute and State University. His areas of research interest are in mathematical optimization modeling, analysis, and the design of algorithms for specially structured linear, nonlinear, and continuous and discrete nonconvex programs. He is a fellow of INFORMS and IIE, and an elected member of the U.S. National Academy of Engineering.



Sastry Kompella (S'04–M'07–SM'12) received the Ph.D. degree in computer engineering from Virginia Polytechnic Institute and State University, Blacksburg, VA, USA, in 2006. He is currently the Head of Wireless Network Theory Section, Information Technology Division, U.S. Naval Research Laboratory, Washington, DC, USA. His research focuses on complex problems in crosslayer optimization and scheduling in wireless and cognitive radio networks.



Jeffrey H. Reed (F'05) received the Ph.D. degree from the University of California, Davis, in 1987. From 2000 to 2002, he was a Director of the Mobile and Portable Radio Research Group. In 2005, he founded Wireless @VT and served as its Director until 2014. He is co-founder of Cognitive Radio Technologies, LLC, and Power Fingerprinting, Inc. He is currently the Willis G. Worcester Professor with the Bradley Department of Electrical and Computer Engineering, Virginia Polytechnic and State University, Blacksburg. His area of expertise is in software radios, cognitive radio, wireless networks, and communications signal processing. He is a Distinguished Lecturer of the IEEE Vehicular Technology Society.